

I-band-like non-dispersive inter-shell interaction induced Raman lines in the D band region of double-walled carbon nanotubes

Bálint Gyimesi · János Koltai · Viktor Zólyomi · Jenő Kürti

Received: date / Accepted: date

Abstract Non-dispersive, inter-layer interaction induced Raman peaks (I bands) – in the region of the D band – have been observed recently for bilayer graphene, when the two layers were rotated with respect to each other. Here, similar observations for double-walled carbon nanotubes (DWCNTs) are theoretically predicted. The prediction is based on double resonance theory, involving non-zone-centered phonons, and the effect of disorder is replaced by interaction between the two tubes.

1 Introduction

Raman spectroscopy is one of the most powerful methods in investigating carbon nanostructures like graphene or carbon nanotubes. The first order Raman spectrum consists of only one band, the G band (in-plane stretching-type motion) for single layer graphene (SLG). In addition to the G band there is another strong band, the RBM (radial breathing mode) for single walled carbon nanotubes (SWCNTs). However, due to higher order processes there are further bands allowed in the Raman spectrum of these materials. Some of them – the D as well as the 2D (with earlier nomenclature G' or D* used for the latter) bands – may even be stronger in intensity as compared to the first order bands.

The origin of the D and 2D bands is revealed by higher order perturbation theory: they arise due to a

fulfilled double resonance condition and involve non- Γ -point phonon(s) [1,2,3,4]. In the case of the D and 2D bands the phonon wave vector (q) is not zero but connects two different virtual intermediate k -points which are in the neighborhood of two different K points in the electronic Brillouin zone (BZ): intervalley process with TO phonons around the K-point. For the 2D band two phonons are involved with opposite wave vector (and same energy). For the D band only one of the two scattering events between these two k -points involves a phonon, the other one is a scattering mediated by a defect. For each fixed q phonon wave vector the Raman amplitude is obtained by integrating appropriate perturbation formulas like

$$\sum_k \frac{M_{rec}(k, -k)M_{def}(k - q)M_{e-ph}(k, q)M_{e-h}(k, -k)}{\Delta E_1 \cdot \Delta E_2 \cdot \Delta E_3} (1)$$

over the virtual intermediate states in the k space [5]. Here M_{e-h} , M_{e-ph} , M_{def} and M_{rec} are the matrix elements corresponding to electron-hole excitation, electron-phonon scattering, electron-defect scattering and electron-hole recombination, respectively. The energy denominators are:

$$\Delta E_1 = E_L - (E_e(k) + E_h(-k)), \quad (2)$$

$$\Delta E_2 = E_L - (E_e(k - q) + E_h(-k) + \hbar\omega(q)), \quad (3)$$

$$\Delta E_3 = E_L - (E_e(k) + E_h(-k) + \hbar\omega(q)). \quad (4)$$

(E_L is the laser excitation energy, and $\hbar\omega(q)$ is the phonon energy.)

The integral is only large if two of the energy denominators become zero simultaneously. This double resonance condition causes the well known dispersion: the shift of the position of the D (and 2D) bands to higher frequencies with increasing laser excitation energy. In

B. Gyimesi · J. Koltai · J. Kürti
Department of Biological Physics, Eötvös Loránd University,
1117 Budapest, Hungary
E-mail: gyimesi.balint.88@gmail.com

V. Zólyomi
Department of Physics, Lancaster University, Bailrigg, Lancaster LA1 4YB, United Kingdom
E-mail: v.zolyomi@lancaster.ac.uk

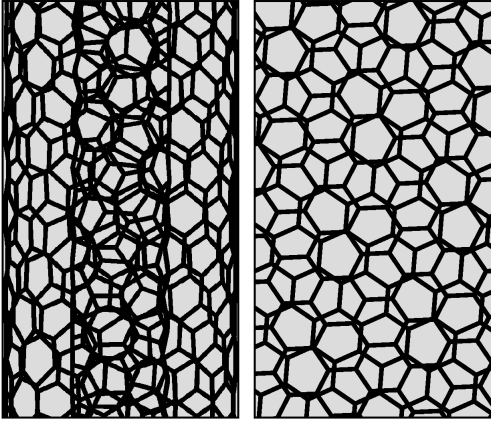


Fig. 1 Side view of the (4,3)@(14,1) double-walled carbon nanotube, and top view of the same DWCNT, unrolled (BL graphene). Since these structures have a similar pattern, the inter-layer interaction may be comparable.

the case of graphene-like materials – due to the Dirac-cones in the electron energy dispersion relation and due to the fact that the frequency of the TO phonons have a minimum at the K-point – the absolute value of the D band maximum lies in the $1300 - 1400 \text{ cm}^{-1}$ range with a slope of the dispersion of $\approx 50 \text{ cm}^{-1}/\text{eV}$. Both the position and the slope of the dispersion are twice as large for 2D band as compared to the D band.

The mechanism for the D and 2D bands in carbon nanotubes is very similar to that in graphene with one essential difference, namely the enhancement effect of the Van Hove (VH) singularities has to be taken into account in the case of nanotubes [2,6].

A different type of peaks in the D band region of the Raman spectrum were observed in bilayer (BL) graphene with rotated layers recently [7,8]. Changing the laser excitation energy changes only the intensity of these bands but not their position. The explanation is based on the interaction between the two layers which can replace the effect of defect scattering. The role of the interaction can be expressed in two different ways. One is to say that one layer imposes a periodic perturbation potential on the other layer with discrete wave vectors which are the Fourier-components of the Moiré pattern of the two rotated hexagonal lattices. The other one is to say that both intermediate scatterings are Umklapp processes, one with the one layer and the other with the other layer. If both layers have the same orientation, that is, the same reciprocal lattice, nothing happens. However, if the two reciprocal lattices differ due to the rotation, the difference of two reciprocal vectors does not map onto the Γ point of the first BZ and therefore this nonzero wave vector has to be taken into account in the (quasi)momentum conservation. In this case there is no continuum for the

possible q vectors but they are discrete. Therefore the positions of so induced lines in the Raman spectrum are fixed, only their intensity, depending on the strength of the double resonance, changes with changing the laser excitation energy. That is, there is no dispersion for these inter-layer interaction induced Raman lines and of course there is no 2D overtone of them, either.

We show in this work that a similar effect can occur in double-walled carbon nanotubes (DWCNTs) if special conditions are fulfilled. The interaction between the inner and outer tubes is similar to the interaction between the two layers in BL graphene and the effect of rotation between the two layers in BL graphene can be replaced by the difference between the chiral angles of the inner and outer tubes. Our work was motivated by recent experimental observations where new non-dispersive lines have been observed in the Raman spectrum of ferrocene-filled carbon nanotubes in the region of the D band, without overtones in the region of the 2D band [9,10]. One stronger line at 1247 cm^{-1} (C_1) and two weaker lines at 1273 cm^{-1} (C_2) and 1361 cm^{-1} (C_3) were observed [11].

In this paper we show theoretically that the interaction between the inner and outer tubes can indeed give rise to the appearance of non-dispersive Raman lines in the D band regime.

2 Theoretical method

The theoretical procedure can be divided into the following three parts.

First, the appropriate wave vector in reciprocal space must be found (connecting the two points determined by each umklapp process). For simplicity we neglect curvature effects for the electronic states. Instead, we use the two dimensional description of the states and processes. The one dimensionality is taken into account only by the well known fact that the allowed states form a set of parallel straight lines, according to the quantization of the component of the wave vectors perpendicular to the tube axis. The reciprocal lattices, both for the inner and for the outer tubes can be mapped onto a common two-dimensional reciprocal space. However, they are rotated with respect to each other according to the difference between the chiral angles of the two tubes. The possible scattering wave vectors can be obtained by the differences between two reciprocal points, one from each of the reciprocal lattices. However, not all possible differences are allowed, only those for which the perpendicular component fulfills the quantization condition. This can only occur if a reciprocal lattice point of one tube fits exactly onto one of the allowed parallel lines of the other nanotube.

Second, the possible wave vectors obtained in the first step are compared to vectors connecting Van Hove singularities in the two-dimensional k space (\mathbf{q}_{VH}). The reason for this is the following. The intensity of the I band depends on the strength of the double resonance. Here, only the effect of the VH enhancement in the intensity is taken into account, similarly to the first quantitative description of the usual D band for carbon nanotubes [2]. The positions of the VH singularities in the two-dimensional k space were obtained using tight-binding (TB) approximation for the electronic dispersion relation.

Third, the phonon frequency for a wave vector satisfying all the necessary conditions described above has to be determined. We calculate the phonon dispersion relations using density functional theory (DFT) in the helical BZ [12,13,14]. These are performed using the VASP code in a plane-wave basis set, using a plane-wave cutoff energy of 500 eV. The details of the DFT calculations can be found in [12,13,14]. The determination of the phonon dispersions are carried out using helical coordinates, therefore, the phonon wave vector from the two-dimensional BZ has to be transformed into its equivalent in the one-dimensional helical BZ.

Further details of the theoretical procedure are explained in the next section as the results are presented.

3 Results and discussions

3.1 Possible phonon wave vectors connecting points of different reciprocal lattices

We use nanotube pairs which differ in their radii approximately by the carbon-carbon Van der Waals equilibrium distance to ensure suitable conditions for interaction. As an example, we choose the (4,3) and the (14,1) chiral indices for the inner and outer nanotubes, respectively. The reason for choosing (4,3) is the motivating experiment mentioned in the introduction. In the experiment the sample had an RBM mode at 470 cm^{-1} with a maximum intensity at about 676 nm laser excitation which corresponds to a Van Hove transition energy of $\approx 1.85 \text{ eV}$ [9, 10]. The (4,3) tube more or less fulfills both conditions: its calculated RBM frequency is 476 cm^{-1} and its calculated E_{11} transition energy is $\approx 1.7 \text{ eV}$.

Fig. 1 shows the reciprocal lattice points of these nanotubes with the allowed momentum-states (k points) of the inner nanotube, which form – according to the quantization condition $2\pi R = \lambda_t n$ of the tangential component of the electron wave number $k_t = \frac{2\pi}{\lambda_t}$, where n is a non-negative integer – a set of parallel straight

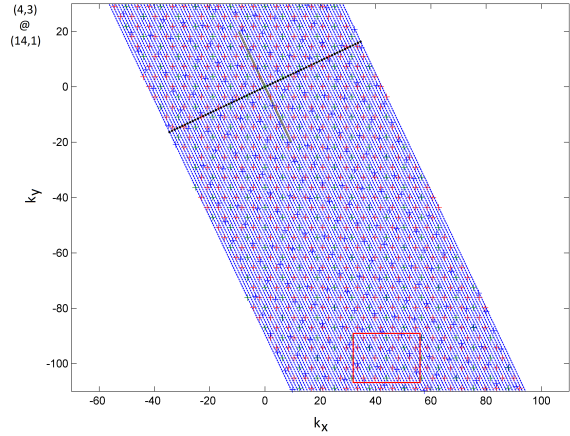


Fig. 2 The two-dimensional representation of the reciprocal lattices of the (4,3) inner and (14,1) outer nanotubes, the vertices of the two-dimensional Brillouin zone (BZ) of the inner nanotube, and the allowed momentum states of the (4,3) nanotube, marked by green, blue and red crosses, and blue dashed lines, respectively. The short black lines and the long grey line are the one-dimensional first BZs of the inner nanotube in linear and helical representation, respectively.

lines with a tilt angle (with respect to the x axis, which is parallel with a Γ -K direction) of

$$\phi = \arccos\left(\frac{n_1 + \frac{n_2}{2}}{\sqrt{n_1^2 + n_1 n_2 + n_2^2}}\right) + \frac{\pi}{2}, \quad (5)$$

where the distance between the neighbouring lines is $1/R$, and n_1, n_2 are positive integers, the chiral indices. R is the radius of the nanotube, which can be expressed with n_1 and n_2 as follows:

$$R = \frac{a_0 \sqrt{n_1^2 + n_1 n_2 + n_2^2}}{2\pi}, \quad (6)$$

where a_0 is the bond length between the carbon atoms (for simplicity, this quantity hereinafter will be considered as unity) [15]. At the bottom of Fig. 2 the red rectangle indicates the surroundings of a reciprocal lattice point of the *outer* nanotube that happens to fit one of the straight lines. Note, that the *inner* nanotube's reciprocal lattice points satisfy this condition automatically. This criterion is the first that must be examined, in order to explain the I band with an interaction process which is connected to the relative chirality of the two shells in the DWCNT.

Fig. 3 is the enlarged version of the previous figure's red framed section, showing a phonon wave vector which can provide potential contributions to the I band. This vector connects such reciprocal lattice points of the inner and outer nanotubes that are in accordance with two important requirements. Firstly, the selection conditions of reciprocal lattice points of the outer nanotube, mentioned above. Secondly, due to the quasi-

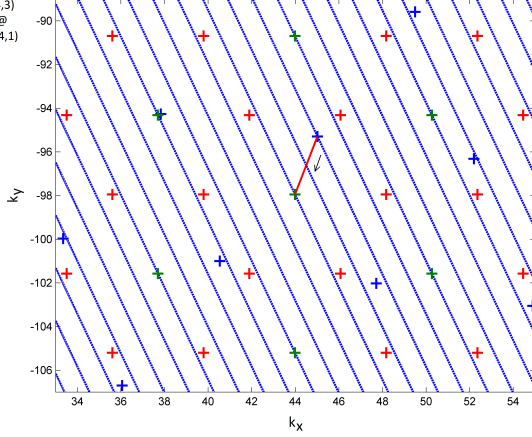


Fig. 3 A reciprocal lattice point - and its narrow surroundings - of the outer nanotube which is precisely matched to the inner nanotube's momentum states (the red highlighted section of Fig. 2). We showed the phonon vector that connects this point to the nearest reciprocal lattice point of the inner nanotube. The orientation of this vector is also included, and marked with a small black arrow. Regarding to the notations, the same convention will be used later.

equivalence of the inner nanotube's reciprocal lattice points, that differ only by reciprocal lattice vectors, it is enough to find the reciprocal lattice point of the inner nanotube which is nearest to the given reciprocal lattice point of the outer nanotube.

We would like to draw attention to another interesting matter. We found that reciprocal lattice points that belong to the outer nanotube, if they satisfy the criteria mentioned above, are always located on the center line (that crosses the origin). Since the nanotubes in the DWCNT are concentric, they have coincident axials, and the slope of the parallel lines - i.e. the allowed momentum states - is identical, too, regardless of chirality. Furthermore, due to the different diameter values, these are following each other with different $1/R$ periodicities that are incommensurate (see Eq. 6), except the trivial cases. This has no effect on the centered line.

It can be shown that the appropriate reciprocal lattice points of the outer nanotube (lying on the center line) can be obtained by a linear combination of the \mathbf{k}_1 and \mathbf{k}_2 reciprocal lattice vectors of the outer tube with coefficients which are integer multiples of the n_1 and n_2 chiral indices of the outer tube: $\mathbf{k}_{hit} = c(n_1\mathbf{k}_1 + n_2\mathbf{k}_2)$. An interesting fact should be mentioned, namely, for a given inner nanotube, when it is only the parity of the outer tube that deviates (i.e. the case of left-handed and right-handed outer nanotubes), the reciprocal lattices of the outer tubes are mirror images of each other with respect to the center line. Therefore \mathbf{k}_{hit} -s remain

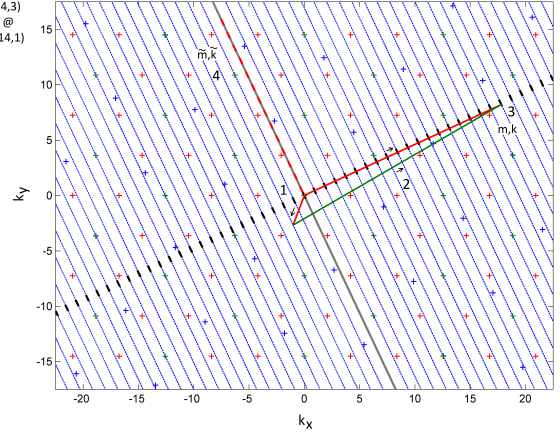


Fig. 4 Transformations of a given phonon wave vector (marked by red lines) to the origin of the 2D BZ (1), and to the linear (3) and helical (4) 1D BZs with a simple shift, a reciprocal lattice vector (2, marked by a green line), and the transformation rules described in the main text, respectively. The linear and helical quantum numbers are referred by the signs showed next to the vectors 3 and 4.

the same, hence there will be no difference regarding to the phonon wave vectors.

Beyond the reciprocal lattice points of the outer nanotube that are lying on the center line, searching for other appropriate reciprocal lattice points is a much more difficult task since we have no analytical formula that could predict the positions of these reciprocal lattice points as a function of the chiral indices. However, the number of such points is very low (or even zero), because of the high probability of incommensurability, according to the lines representing the allowed momentum states.

The next step in searching for the positions of the lines of the I band is to determine the frequencies corresponding to the phonon wave vectors. Our goal is to obtain the helical quantum numbers of a wave vector so that they can be used for the one-dimensional helical phonon dispersion calculated using density functional theory in the helical Brillouin zone [12, 13, 14]. The procedure can be viewed on Fig. 4. We perform transformations that are necessary to determine the linear and finally the helical quantum numbers which are connected to a given phonon wave vector [16]. First of all, we move the phonon wave vector shown in Fig. 3 to the origin, into the 1st BZ of the two-dimensional reciprocal space (1). Then - by adding a suitable reciprocal lattice vector (2) - we map the vector into the one-dimensional linear BZ (that is onto one of the 74 short lines of the momentum space, in the case of the (4,3) tube), in order to get the appropriate quantum numbers m and k (3) and from these the helical ones \tilde{m} and \tilde{k} (4). The linear

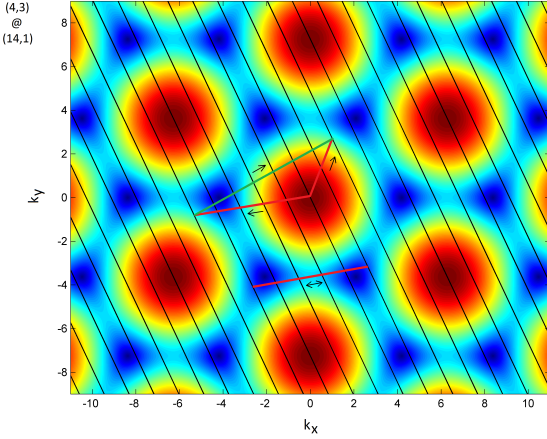


Fig. 5 Tight-binding electron dispersion relation $t_0 \sqrt{1 + 4 \cos \frac{k_x}{2} \left(\cos \frac{k_x}{2} \cos \frac{\sqrt{3}k_y}{2} \right)}$, where $t_0 = 2.9$ eV, and k_x, k_y are the wave vector components corresponding to the direction of the axes, respectively, the allowed states of the momentum space of the (4,3) nanotube (solid black lines), and a transformed transition vector (\mathbf{q}_{VH}) which connects two Van Hove singularities. (Note, that there are multiple VH singularities, but for the sake of simplicity, we focus only on one of them.)

and helical quantum numbers can be transformed into each other by the following equations:

$$|\tilde{k}, \tilde{m}\rangle = \left| k + \frac{wm}{n} \frac{2\pi}{a} + \tilde{K}, \frac{2\tilde{\pi}}{a} m + \tilde{M}n \right\rangle, \quad (7)$$

$$|k, m\rangle = \left| \tilde{k} - \frac{w\tilde{m}}{n} \frac{2\pi}{a} + K \frac{2\pi}{a}, \tilde{m} - Kp + Mq \right\rangle \quad (8)$$

where \tilde{K}, \tilde{M}, K and M are integers determined by the condition that the quantum numbers are in the intervals

$$k \in \left(-\frac{\pi}{a}, \frac{\pi}{a} \right], m \in \left(-\frac{q}{2}, \frac{q}{2} \right], \quad (9)$$

$$\tilde{k} \in \left(-\frac{q}{n} \frac{\pi}{a}, \frac{q}{n} \frac{\pi}{a} \right], \tilde{m} \in \left(-\frac{n}{2}, \frac{n}{2} \right]. \quad (10)$$

In these equations, $\tilde{\pi} = \frac{\pi q}{n}$, q is the number of graphene lattice points in the nanotube unit cell, n is the number of lattice points on the chiral vector (the greatest common divisor, g.c.d., of the components of the chiral vector), a is the translational period of the nanotube, while parameters w and p are non-trivial functions of the chiral indices [17, 15].

3.2 The role of Van Hove singularities

There is one important difference between two-dimensional graphene and one-dimensional nanotubes: the existence of Van Hove singularities in the density of states in the latter case. This has an important consequence: there is

an extra enhancement in intensity if the phonon wave vector connects two k points so that both of them correspond to a VH singularity [2]. Remaining in the two-dimensional picture: the position of the VH singularities in the two-dimensional BZ can be found where one of the allowed parallel lines touches an equi-energy curve, that is, perpendicular to the energy gradient. These particular transitions – according to the double resonance condition – must connect points in the reciprocal space that have the same energy (or at most differ only by the energy of one phonon). Fig. 5 shows such a transition. The number of transition is greatly reduced by the criteria that the allowed momentum states of the nanotubes are limited to the parallel lines, the perpendicularity condition of the energy gradient applied to these lines, and the symmetry induced equivalence of the reciprocal space points. Since the Van Hove singularities have a comparable amplification factor to the double resonance – regarding to the intensity – it is enough to use a similarity measure for a given phonon vector (that may give a contribution to the I band) that is based on these aspects. In other words, only the phonon wave vectors connecting a reciprocal lattice point of the inner tube with a reciprocal lattice point of the outer tube, as discussed in the previous subsection, can give rise to large enough intensity, which matches or almost matches a \mathbf{q}_{VH} wave vector between two VH singularity points. Accordingly, we define the following phenomenological quantity:

$$C_I = e^{-\frac{(\mathbf{q} - \mathbf{q}_{VH})^2}{c^2 |\mathbf{q}_0|^2}} \quad (11)$$

where \mathbf{q} and \mathbf{q}_0 belongs to the actual transition and to the vector which connects the inequivalent K and K' trigonal points, respectively. This formula brings information about the magnitude of the contributions to the I band. The value of the constant c – which is a kind of normalization factor – has been set to 0.1. In order to perform the comparison, we made the shift to the origin again, followed by a transformation with a reciprocal lattice vector to move the Van Hove vector to the first Brillouin zone (see Fig. 5). Note, that the determination of the positions of the VH singularities was carried out without taking into account curvature effects (relying on the two-dimensional tight-binding approximation for electron energies combined with the discrete parallel lines for the allowed wave vectors.). Of course, considering σ - π rehybridization due to the curvature would influence strongly the electron energies [18] and therefore also \mathbf{q}_{VH} if the nanotubes have small diameters.

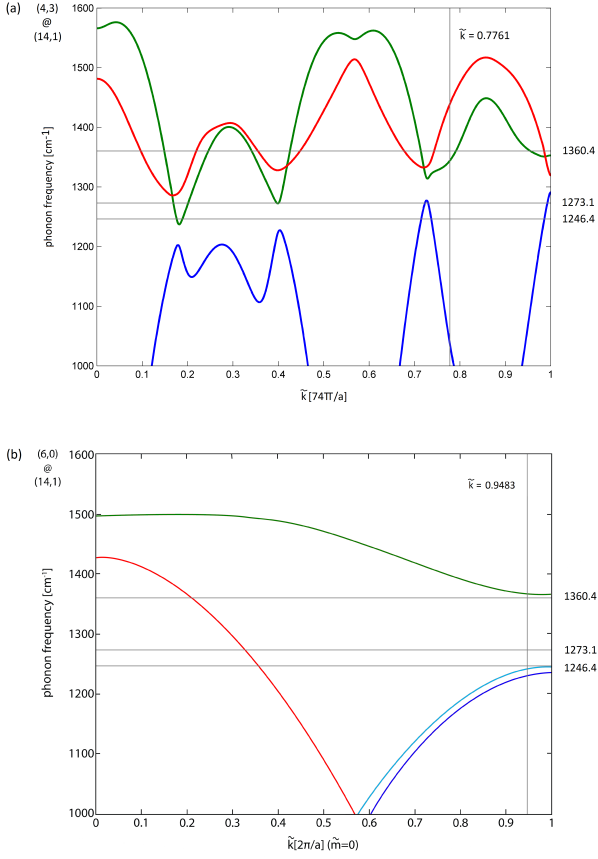


Fig. 6 Phonon dispersions of the (4,3) (a) and (6,0) (b) nanotube (calculated via DFT), which are characterized by the $\tilde{m} = 0$ helical quantum number. The vertical grey lines represent the helical wave numbers that have been specified in the reciprocal space of the (4,3) and (6,0) inner and (14,1) outer nanotubes.

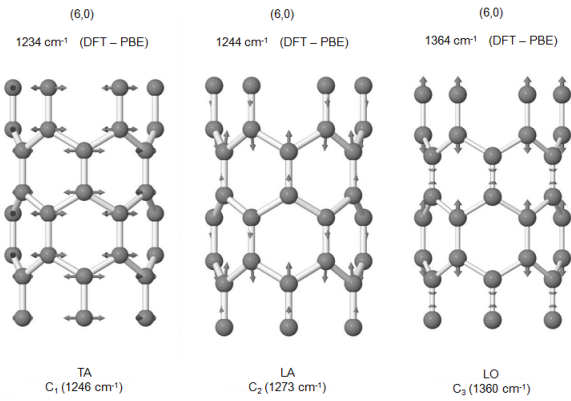


Fig. 7 Certain vibrations of the (6,0) nanotube, calculated via DFT Perdew-Burke-Ernzerhof model. The TA, LA and LO abbreviations correspond to transverse and longitudinal acoustic and optical modes, respectively.

3.3 I band frequencies

After finding the possible combinations of reciprocal vectors of the inner and outer tubes one has to compare them with the \mathbf{q}_{VH} Van Hove vector and consider only those q values for which the C_I quantity as defined in Eq. 11 is close to unity. All these conditions together are rather strict so the number of the wave vector candidates for the I band is small. In fact, for the case of (4,3)@(14,1) we found only one such wave vector. After the appropriate transformations (as shown in Fig. 3) we obtained $\tilde{k} = 0.7761$ for the helical wave number of this vector. (The \tilde{m} quantum number is zero, because the g.c.d. is one for (4,3).) For comparison, the quantum number for the Van Hove vector is $\tilde{k}_{VH} = 0.7762$ for (4,3).

Fig. 6a shows the DFT calculated phonon dispersion of (4,3) nanotube in the helical BZ. The vertical grey line shows the position of the $\tilde{k} = 0.7761$ helical wave number. This line intersects three phonon dispersion curves. The three horizontal grey lines represent the measured frequencies mentioned in the Introduction, for comparison. It can be seen that although one of the obtained frequencies matches quite well the measured 1360 cm^{-1} , the other two calculated values are far away from the measured ones.

We repeated the whole procedure for another combination: (6,0)@(14,1). The diameter as well as one of the Van Hove excitation energies of the (6,0) nanotube is very similar to those of the (4,3) tube (see Fig. 6 in Ref. [9]). For the zig-zag (6,0) nanotube it is easy to show that the \tilde{k}_{VH} vector connecting two VH singularities has $m = 6$ and $k = 0$ linear quantum numbers which transforms into $\tilde{m} = 0$ and $\tilde{k} = 1$ helical quantum numbers. We found a q vector between the reciprocal points of the inner and outer tubes which is very close to the aforementioned \tilde{k}_{VH} vector. Its helical wave number is $\tilde{k} = 0.9483$.

Fig. 6b shows the DFT calculated phonon dispersion of (6,0) nanotube in the helical BZ (for $\tilde{m} = 0$). The vertical grey line shows the position of the $\tilde{k} = 0.9483$ helical wave number. The three horizontal grey lines represent again the measured frequencies mentioned in the Introduction. It can be seen that the so obtained frequencies are quite close to the measured ones.

Fig. 7a shows the vibrational pattern for these three normal modes. The two with lower frequencies would be degenerate in the planar case. The curvature results in a small splitting of their frequencies.

4 Conclusions

In conclusion, we have shown that similar to the appearance of the non-dispersive Raman D band activated by well-ordered inter-layer interactions in rotationally stacked bilayer graphene (I band) the interaction between the inner and outer tubes with different chiralities can result in the appearance of non-dispersive I band in double-walled carbon nanotubes as well.

We have shown on the examples of (4,3)@(14,1) and (6,0)@(14,1) DWCNTs that the strict conditions for appropriate wave vectors for inducing the non-dispersive I band in the D band region can be fulfilled. We focused on the most important factor, namely that the difference between two reciprocal lattice points – one for the inner and one for the outer tube – matches or nearly matches a vector connecting two VH singularities in k space. Of course the double resonance condition is only fulfilled for the laser excitation energy which matches the VH transition energy. Interestingly, the enantiomers can not be distinguished, because the interaction which results in the I band of a given inner tube with the left handed and with the right handed form of the outer tube of the same chirality turned out to be exactly the same.

There are further factors which influence the intensity of the I band, namely the matrix elements, of which the most important is the electron-phonon coupling constant. This will however only be important for the exact intensity of the non-dispersive line; neglecting the matrix elements therefore does not impact the message of this work, namely that the appearance of I-band-like lines is possible in DWCNTs.

Acknowledgements Support from the Hungarian National Research Fund (OTKA), grant numbers K81492 and K108676 are gratefully acknowledged.

References

1. C. Thomsen and S. Reich, Double resonant Raman scattering in graphite, *Phys. Rev. Lett.*, 85, 5214 (2000)
2. J. Kürti, V. Zólyomi, A. Grüneis, and H. Kuzmany, Double resonant Raman phenomena enhanced by Van Hove singularities in single-wall carbon nanotubes, *Phys. Rev. B*, 65, 165433 (2002)
3. P. Venezuela, M. Lazzeri, and F. Mauri, Theory of double-resonant Raman spectra in graphene: Intensity and line shape of defect-induced and two-phonon bands, *Phys. Rev. B*, 84, 035433 (2011)
4. V. Zólyomi, J. Koltai, and J. Kürti, Resonance Raman spectroscopy of graphite and graphene, *physica status solidi (b)*, 248, 2435–2444 (2011)
5. R. Martin and L. Falicov, Resonant Raman scattering, in: *Light Scattering in Solids I, Topics in Applied Physics*, Vol. 8 (Springer Berlin Heidelberg, 1983), pp. 79–145.
6. J. Laudénbach, F. Hennrich, H. Telg, M. Kappes, and J. Maultzsch, Resonance behavior of the defect-induced Raman mode of single-chirality enriched carbon nanotubes, *Phys. Rev. B*, 87, 165423 (2013)
7. A. K. Gupta, Y. Tang, V. H. Crespi, and P. C. Eklund, Nondispersive Raman D band activated by well-ordered interlayer interactions in rotationally stacked bilayer graphene, *Phys. Rev. B*, 82, 241406(R) (2010)
8. A. Righi, S.D. Costa, H. Chacham, C. Fantini, P. Venezuela, C. Magnuson, L. Colombo, W.S. Bacsá, R.S. Ruoff, and M.A. Pimenta, Graphene Moiré patterns observed by umklapp double-resonance Raman scattering, *Phys. Rev. B*, 84, 241409(R) (2011)
9. W. Plank, R. Pfeiffer, C. Schaman, H. Kuzmany, M. Calvarasi, F. Zerbetto, and J. Meyer, Electronic Structure of Carbon Nanotubes with Ultrahigh Curvature, *ACS Nano* 4, 4515 (2010)
10. X. Liu, H. Kuzmany, T. Saito, and T. Pichler, Temperature dependence of inner tube growth from ferrocene-filled single-walled carbon nanotubes, *physica status solidi (b)*, 248, 2492–2495 (2011)
11. H. Kuzmany, private communication
12. V. Zólyomi, J. Koltai, J. Kürti, and H. Kuzmany, Phonons of single walled carbon nanotubes, in: *DFT Calculations on Fullerenes and Carbon Nanotubes*, edited by V. Basiuk and S. Irle, (Signpost Publisher, Kerala, India, 2008)
13. J. Koltai, V. Zólyomi, and J. Kürti, Phonon dispersion of small diameter semiconducting chiral carbon nanotubes – a theoretical study, *physica status solidi (b)*, 245, 2137–2140 (2008)
14. Á. Ruzsnyák, J. Koltai, V. Zólyomi, and J. Kürti, Using line group theory for the symmetry assignment of the phonons of single walled carbon nanotubes, *physica status solidi (b)*, 2456, 2614–2617 (2009)
15. S. Reich, C. Thomsen and J. Maultzsch, *Carbon Nanotubes, Basic Concepts and Physical Properties*, Wiley-VCH, Weinheim (2004)
16. E. Dobardžić, I. Milošević, T. Nikolić, T. Vuković, and M. Damnjanović, Single-wall carbon nanotubes phonon spectra: Symmetry-based calculations, *Phys. Rev. B*, 68, 045408 (2003)
17. M. Damnjanović, I. Milošević, T. Vuković, and R. Sredanović, Full symmetry, optical activity, and potentials of single-wall and multiwall nanotubes, *Phys. Rev. B*, 60, 2728–2739 (1999)
18. V. Zólyomi and J. Kürti, First-principles calculations for the electronic band structure of small diameter single-wall carbon nanotubes, *Phys. Rev. B*, 70, 085403 (2004)